Supporting Information

A Hundredfold Enhancement of Relaxation Times among Er(III) Single-Molecule Magnets with Comparable Energy Barriers

Qi-Wei Chen,[a,b] You-Song Ding,[b,c,*] Tianjiao Xue,[b,c] Xiao-Fei Zhu[a,*] and Zhiping Zheng[b,c,*]

[a] School of Chemistry and Life Science, Changchun University of Technology, Changchun 130012, China. zhuxiaofei@ccut.edu.cn

[b] Department of Chemistry, Southern University of Science and Technology, Shenzhen, Guangdong 518055, China. dingys@sustech.edu.cn; zhengzp@sustech.edu.cn.

[c] Key University Laboratory of Rare Earth Chemistry of Guangdong, Southern University of Science and Technology, Shenzhen, Guangdong 518055.

Table S1 Comparison of the relaxation times for [K(18-C-6)][Er(COT)$_2$], [K(18-C-6)(THF)$_2$][Er(COT)$_2$] [1] and **3**.

[K(18-C-6)][Er(COT)$_2$]		[K(18-C-6)(THF)$_2$][Er(COT)$_2$]		**3**	
27.0	1.81E-04	27.0	1.83E-04		
26.5	2.17E-04	26.5	2.20E-04		
26.0	2.61E-04	26.0	2.63E-04		
25.5	3.13E-04	25.5	3.17E-04		
25.0	3.80E-04	25.0	3.82E-04		
24.5	4.60E-04	24.5	4.64E-04		
24.0	5.62E-04	24.0	5.66E-04		
23.5	6.87E-04	23.5	6.93E-04		
23.0	8.48E-04	23.0	8.55E-04		
22.5	0.00105	22.5	0.00106		
22.0	0.00131	22.0	0.00132		
21.5	0.00160	21.5	0.00165		
21.0	0.00208	21.0	0.00210		
20.5	0.00266	20.5	0.00269		
20.0	0.00343	20.0	0.00346		
19.5	0.00448	19.5	0.00453		
19.0	0.00593	19.0	0.00597		
18.5	0.00792	18.5	0.00799		
18.0	0.01076	18.0	0.01086		
17.5	0.01480	17.5	0.01500		
17.0	0.02080	17.0	0.02090	17	2.38E-04
16.5	0.02970	16.5	0.02980	16.5	3.04E-04
16.0	0.04310	16.0	0.04350	16	5.45E-04
15.5	0.06400	15.5	0.06400	15.5	8.21E-04
15.0	0.09500	15.0	0.09500	15	0.00109
14.5	0.14700			14.5	0.00187
14.0	0.23400			14	0.00283
13.5	0.38600			13.5	0.00439
13.0	0.61900			13	0.00705
				12.5	0.01172
				12	0.02053
				11	0.06574
				10	0.2222
				9	0.75414

Table S2 Comparison of the relaxation times for $[K(DME)_2][Er(COT^{TBS2})_2]$, $[K(18\text{-}C\text{-}6)(THF)_2][Er(COT^{TBS2})_2]$, $[K(2,2,2\text{-cryptand})][Er(COT^{TBS2})_2]$ [2], **1** and **2**.

$[K(DME)_2][Er(COT^{TBS2})_2]$		$[K(18\text{-}C\text{-}6)(THF)_2]$ $[Er(COT^{TBS2})_2]$		$[K(2,2,2\text{-cryptand})]$ $[Er(COT^{TBS2})_2]$		**2**	
						23	1.07842E-4
						22.5	1.49595E-4
						22	1.86232E-4
						21.5	1.98836E-4
21	2.53E-04					21	2.52186E-4
				20.5	1.86E-04	20.5	3.251E-4
20	4.26E-04			20	2.26E-04	20	3.98529E-4
				19.5	2.79E-04	19.5	5.2858E-4
				19	3.49E-04	19	6.71548E-4
		18.5	1.81E-04	18.5	4.40E-04	18.5	9.1751E-4
18	0.00137	18	2.30E-04	18	5.63E-04	18	0.00119
		17.5	3.06E-04	17.5	7.30E-04	17	0.00223
17	0.00262	17	4.21E-04	17	9.65E-04	16	0.00456
		16.5	5.80E-04	16.5	0.0013	15	0.01018
16	0.00537	16	8.29E-04	16	0.00179		
		15.5	0.0012	15.5	0.00252		
		15	0.00179	15	0.00367	15	0.01018
14	0.02909	14	0.00406	14	0.00941	14	0.02544
		13	0.0106	13	0.02327	13	0.07019
12	0.24433	12	0.0322	12	0.06939		
		11	0.11581	11	0.27698	11	0.83004
		10	0.48177				

Table S3, Reported Er-COT single molecule magnets with different substituted groups.

	R	Compound	U_{eff} / K	T_B / K	T_H / K	Ref
COT^{2-}		[Cp*ErCOT]	323 (0 Oe) 197 (0 Oe)	4.6	5	3
		$[K(18\text{-}C\text{-}6)][Er(COT)_2]$	211 (0 Oe)	10.1	10	1
		$[K(18\text{-}C\text{-}6)(THF)_2][Er(COT)_2]$	211 (0 Oe)	-	10	1
		$[K(18\text{-}C\text{-}6)][Er(COT)_2]$	286 (0 Oe)	-	12	4
		$K_2(THF)_4[Er_2(COT)_4]$	306 (0 Oe)	12.9	12	5
		$[(C_5H_5BH)Er(COT)]$	371 (0 Oe)	-	8	6
		$[(C_5H_5BMe)Er(COT)]$	421 (0 Oe)	-	6	6
		$[(C_5H_5BNEt_2)Er(COT)]$	250 (0 Oe)	-	-	6
		$[Er(\mu_2\text{-}Cl)(COT)(THF)]_2$	162 (0 Oe)	-	4	7
		[{(*S*)-PETA}Er(COT)(THF)]	50 (0 Oe)	-	-	8
		(Dsp)Er(COT)	358	8.5	9	9
		$Er(COT)I(THF)_2$	137 (0 Oe)			10
		$Er(COT)I(Py)_2$	148 (0 Oe)			10
		$Er(COT)I(MeCN)_2$	154 (0 Oe)			10
		Er(COT)(Tp*)	192 (0 Oe)			10
		Er(COT)I(DMPE)	108 (0 Oe)	-	-	11
		$[Er(COT)(\mu\text{-}I)]_2(\mu\text{-}DPPE)$	264 (0 Oe)	-	-	11
		$[Er(COT)(\mu\text{-}I)]_2(\mu\text{-}DPPM)$	290 (0 Oe)	-	-	11
		$[Er(COT)(\mu\text{-}I)(MDPP)]_2$	253 (0 Oe)	-	-	11
		[(LOMe)Er(COT)]	111			12
		$[(THF)_2(OAr)Er(COT)]$	55			12
		$[(C_9H_9)Er(COT)]$	361 (0 Oe)	-	10	13
		$[Er(COT)(\mu\text{-}OEt)(THF)]_2$	27 (0 Oe) 52 (800 Oe)	-	-	14
		$[Er(COT)]_2(\mu\text{-}O^tBu)_2(THF)$	9 (0 Oe) 31 (2 kOe)	-	-	14
		$[Li(DME)_3][BoEr(COT)]$	157 (0 Oe)		2	15
		$[ErKCa(COT)_3(THF)_3]$	287 (0 Oe)	-	10	16
		$(COT)Er(Cp^{ttt})$	228 (0 Oe)			17
		$[Er(THF)_3(COT)][C_9H_9]$	97 (0 Oe)			18
COT^{R2}	TMS	$[Li(DME)_3][Er(COT^{TMS2})_2]$	187 (0 Oe)	8	8	19
		$[Er_2(COT^{TMS2})_3]$	323 (0 Oe)	12.5	14	5
	TIPS	$[Li(THF)(L^{Pb})Er(COT^{TIPS2})]$	145 (0 Oe)	6.1	6.1	20
		$[Li(12\text{-}C\text{-}4)_2(L^{Pb})Er(COT^{TIPS2})]$	61 (0 Oe)	2.8	2.8	20
		$Er(COT^{TIPS2})I(THF)_2$	118 (0 Oe)	-	-	21
		$[Er(COT^{TIPS2})(\mu\text{-}I)(THF)]_2$	198 (0 Oe) 218 (0 Oe)	-	-	21
		$[Er_3(COT^{TIPS2})_3(\mu_2\text{-}I)(\mu_3\text{-}I)_2]$	200 (0 Oe)	-	-	21

			243 (0 Oe) 282 (0 Oe)			
	TBS	$[K(DME)_2][Er(COT^{TBS2})_2]$	190 (0 Oe)	10	10	2
		$[K(18\text{-}C\text{-}6)(THF)_2]$ $[Er(COT^{TBS2})_2]$	171 (0 Oe)	9	9	2
		$[K(2,2,2\text{-cryptand})]$ $[Er(COT^{TBS2})_2]$	166 (0 Oe)	9	11	2
COT^{R4}	hex	$[K(18\text{-}C\text{-}6)][Er(hdcCOT)_2]$	212 (0 Oe)	-	-	22

Abbreviation

Cp* = pentamethylcyclopentadienide

18-C-6 = 18-Crown-6

(*S*)-PETA = (*S*,*S*)-*N*,*N*′-bis(1-phenylethyl) pivalamidinate

Dsp^{-} = 3,4-dimethyl-2,5-bis(trimethylsilyl)phospholyl)

Py = pyridine

MeCN = acetonitrile

Tp* = tris(3,5-dimethyl-1-pyrazolyl)borate

DMPE = 1,2-bis(dimethylphosphino)ethane

DPPE = 1,2-bis(diphenylphosphino)ethane

DPPM = 1,2-bis(diphenylphosphino)methane

MDPP = methyldiphenylphosphine

LOMe = $[(\eta^5\text{-}C_5H_5)Co\{P(=O)(OMe)_2\}_3]$, COT = cyclooctatetraenyl)

Ar = 2,6-$Dipp_2C_6H_3$, Dipp = 2,6-diisopropylphenyl

Bo = benzoborole dianion

$(Cp^{ttt})^{-}$ = 1,2,4-tri(tert-butyl)cyclopentadienide

L^{Pb} = 1,4-bis-*tert*-butyl-dimethylsilyl-2,3-bis-phenyl-plumbolyl

COT^{TIPS2} = 1,4-bis-triisopropylsilyl-cyclooctatetraenyl

12-C-4 = 12-Crown-4

COT^{TBS2} = 1,4-$(^{t}BuMe_2Si)_2C_8H_6$

hdcCOT = hexahydrodicyclopentacyclooctatetraenide dianion

General synthetic consideration

All manipulations are carried out under standard Schlenk techniques or glove box under an argon atmosphere. All glassware was dried overnight at 120°C before use. Anhydrous THF was purchased from energy-chemical, while n-hexane was dried using activated alumina and stored over Potassium mirror before use. Anhydrous $ErCl_3$ [23], cyclooctatetraene (COT) [24], bromocyclooctatetraene (BrCOT) [25], Trimethylsilylcyclooctatetraene (COT^{TMS1}) [26], 5,8-bis(trimethylsilyl)-l,3,6-cyclooctatriene (H_2COT^{TMS2}) [27]), and 1.3,6,6-tetrakis(trimethylsilyl)cyclooctatriene (COT^{TMS4}) [27] were synthesized using a previously published procedure. All other reagents were purchased from energy-chemical and used without further purification. Elemental analyses were recorded on a Carlo Erba EA1110 simultaneous CHN elemental analyzer. FT-IR spectra were recorded in the range 600 - 4000 cm^{-1} on a Bruker tensor II spectrophotometer with ATR mode.

Synthesis

Scheme S1 synthesis of the three Cyclooctatetraenide dianions.

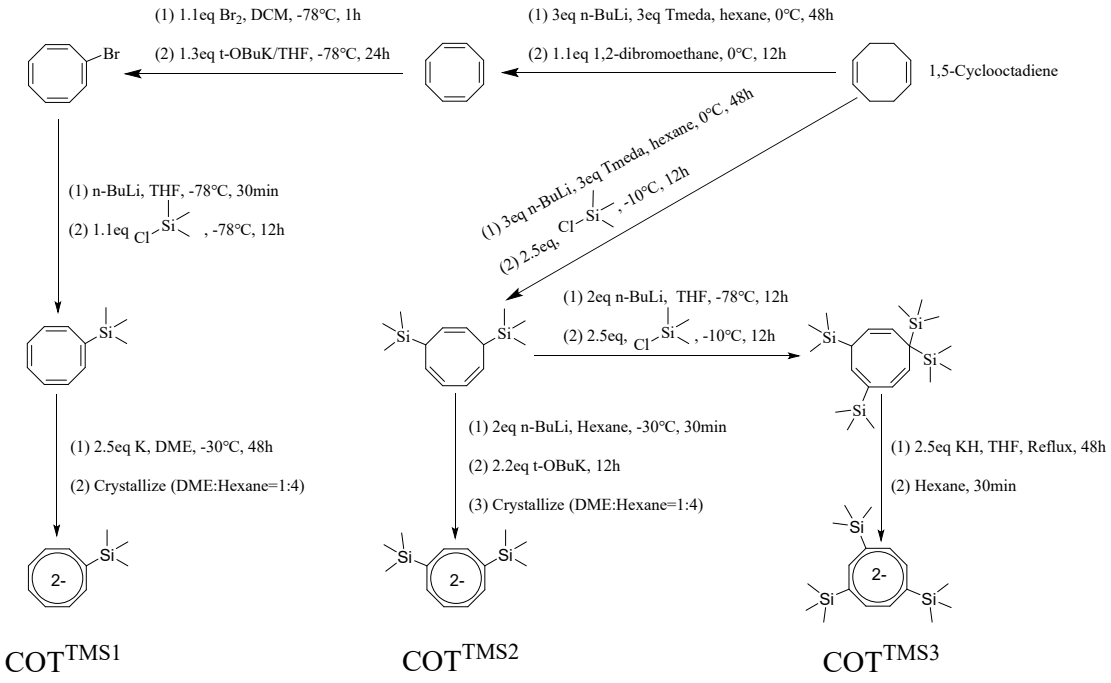

Experimental Section

The synthesis of $K_2(DME)_2COT^{TMS}$ ($K_2(COT^{TMS1})$)

Complex **$K_2(COT^{TMS1})$** was prepared by following the typical procedure to reduce COT [28]. Under argon atmosphere, COT^{TMS} (5.28 g, 30 mmol) was added to a solution of freshly cut potassium (2.93 g, 75 mmol) in DME (60 mL) at -30 ℃. The temperature was then slowly rise to room temperature and the dark red solution was stirred for 48 hours. The mixture was filtrated in the glovebox to remove excess potassium. Colorless crystals for **$K_2(COT^{TMS1})$** was obtained in the mixed solution of DME and hexane (1:4) with the yield of 37%. Found: C, 52.2; H, 8.5. Calc. for $C_{19}H_{36}K_2O_4Si$: C, 52.5; H, 8.5%.

The synthesis of $K_2(DME)_2COT^{TMS2}$ ($K_2(COT^{TMS2})$)

Complex **$K_2(COT^{TMS2})$** was prepared according to the literature procedure with slight modifications as follow [20]. Under argon atmosphere, *n*-BuLi (25.5 mL, 63.86 mmol) was added to dry hexane (100 mL) solution of H_2COT^{TMS2} (8 g, 31.93 mmol) at -30 ℃ and stirred for 30 minutes. KO^tBu (7.88 g, 70.25 mmol) was then added to the mixture. The resulting solution was stirred overnight at the room temperature. The mixture was then filtrated and the residue was then washed with plenty of hexane solution until the filtrate become colorless. Recrystallization of the residue from mixed solution of DME and hexane (1:4) yield colorless crystals for **$K_2(COT^{TMS2})$**. Yield 55%. Found: C, 51.6; H, 9.3. Calc. for $C_{22}H_{44}K_2O_4Si_2$: C, 52.1; H, 8.8%. Note: The 1,4-silylate COT in **$K_2(COT^{TMS2})$** changed to the 1,3-analogue **$K_2(COT^{TMS2})$,** which also taken place when prepared by reaction of H_2COT^{TMS2} with KH [29].

The synthesis of $K_2(THF)_3COT^{TMS3}$ ($K_2(COT^{TMS3})$)

Complex **$K_2(COT^{TMS3})$** was prepared according to the literature procedure [27]. At the argon atmosphere, KH (4.44 g, 110.79 mmol) was added to the solution of H_2COT^{TMS4} (17.50 g, 44.32 mmol) in dry THF (100 mL) at room temperature, and then the mixture was heated to reflux for 48 hours. Subsequently, excess KH was filtered off, the solvent was removed under vacuum, and the residue taken up in hexane (40 mL) and stirred for 3 hours. The white solid precipitate was separated with the yield of 36%. Colorless crystals for **$K_2(COT^{TMS3})$** were obtained by diffraction of hexane

to saturated THF solution of **$K_2(COT^{TMS3})$** at room temperature. Found: C, 56.5; H, 9.1. Calc. for $C_{29}H_{56}K_2O_3Si_3$: C, 56.6; H, 9.2%.

The synthesis of $(COT^{TMS})Er(COT^{TMS})K(DME)_2$ (1)

At the argon atmosphere, $ErCl_3$ (0.134 g, 0.5 mmol) and **$K_2(COT^{TMS1})$** (0.434 g, 1 mmol) was dispersed in DME (10 mL) and stirred for 48 hours at room temperature. After filtration, the solvent was removed under vacuum, and the residue was washed with hexane and then dissolved in DME (*ca.* 1 mL). The solution was cooled to -35 ℃ overnight to give orange crystals for **1** that collected by filtration. The yield is 39%. IR: ν [cm^{-1}] = 3037 (w), 2944 (w), 2892 (w), 1561 (w), 1499 (w), 1443 (w), 1400 (w), 1375 (w), 1243 (s), 1181 (w), 1023 (m), 925 (m), 831 (s), 811 (m), 748 (m), 702 (s), 630 (m), 585 (w), 536 (w). Found: C, 49.2; H, 6.6. Calc. for $C_{30}H_{52}ErKO_4Si_2$: C, 48.7; H, 7.1%.

The synthesis of $(COT^{TMS2})Er(COT^{TMS2})K(DME)_2$ (2)

Complex **2** was prepared by the same method as **1**, using $ErCl_3$ (0.134 g, 0.5 mmol) and **$K_2(COT^{TMS2})$** (0.506 g, 1 mmol). Orange crystals of **2** were obtained by cooling saturated DME solution of **2** overnight. The yield is 36%. IR: ν [cm^{-1}] = 3038 (w), 2949 (w), 2895 (w), 1441 (w), 1401 (w), 1244 (s), 1210 (w), 1047 (s), 979 (w), 931 (m), 907 (w), 825 (s), 782 (w), 731 (s), 682 (m), 631 (m), 551 (m). Found: C, 48.8; H, 8.0. Calc. for $C_{36}H_{67}ErKO_4Si_4$: C, 49.0; H, 7.7%. Note: 1,3- silylate COT in **$K_2(COT^{TMS2})$** changed backed to the 1,4-analogue when coordinated to the lanthanide ions, probably because the TMS groups can wander to neighbor carbon when coordinated to lanthanide ions [30].

The synthesis of $[(COT^{TMS3})Er(COT^{TMS3})K(18\text{-Crown-}6)_{1.5}(DME)]\cdot DME$ (3)

At the argon atmosphere, $ErCl_3$ (0.134 g, 0.5 mmol) and **$K_2(COT^{TMS3})$** (0.506 g, 1 mmol) was dispersed in DME (10 mL) and stirred for 24 hours at 80 ℃. After filtration, 18-crown-6 (0.264 g, 1 mmol) was added to the filtrate and the mixture was stirred at room temperature overnight. The mixture was filtrated again and the solvent was removed under vacuum. The residue was washed with hexane and then dissolved in DME (1 mL). The DME solution was cooled to -35 ℃ overnight to yield orange crystals of **3**. The yield is 26%. IR: ν [cm^{-1}] = 3016 (w), 2946 (w), 2892 (w), 1536 (w),

1471 (w), 1452 (w), 1402 (w), 1350 (w), 1284 (w), 1239 (m), 1102 (s), 1069 (m), 983 (w), 960 (w), 935 (w), 863 (w), 825 (s), 744 (s), 677 (w), 634 (m), 548 (w), 529 (w), 508 (w). Found: C, 50.9; H, 8.6. Calc. for $C_{60}H_{119}ErKO_{13}Si_6$: C, 50.6; H, 8.4%.

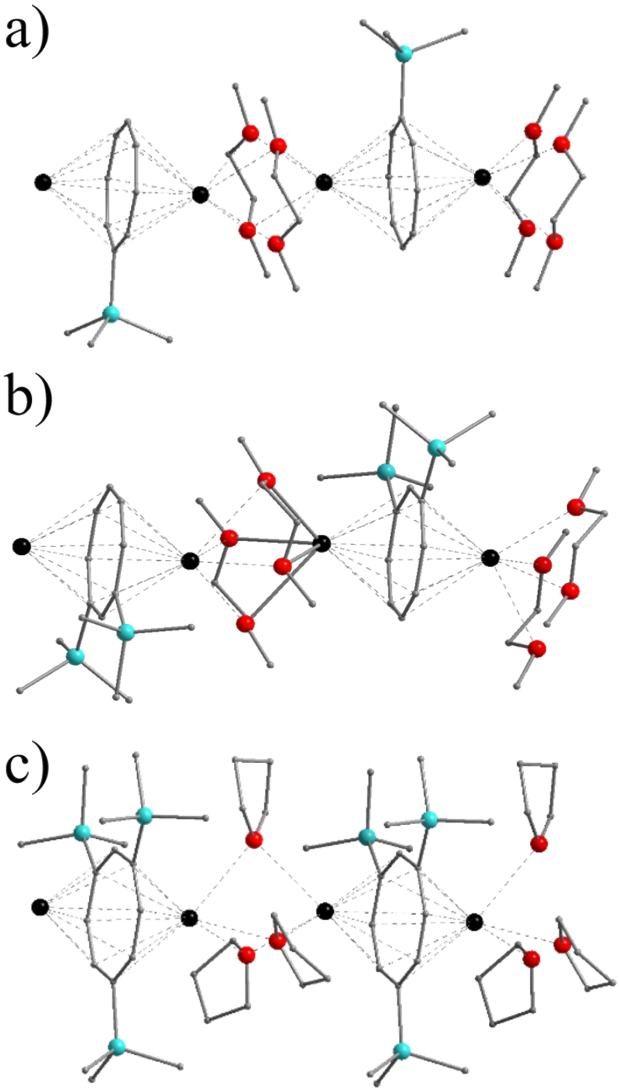

Figure S1 The crystal structure of complexes **$K_2(COT^{TMS1})$** (a), **$K_2(COT^{TMS2})$** (b) and **$K_2(COT^{TMS3})$** (c). Other atoms are omitted for clarity. Colour code: dark red (K), red (O), orange (Si), white (C).

Crystallography

Single-crystal X-ray diffraction studies were carried out with the use of a Bruker D8 VENTURE diffractometer with Mo-Kα radiation (λ = 0.71073 Å) at 100 K. Using Olex2 [31], the structures were solved with the SHELXT [32] structure solution program using Intrinsic Phasing and refined with the SHELXL [33] refinement package using Least Squares minimization. All hydrogen atom positions were generated geometrically and refined with isotropic temperature factors. Cambridge Crystallographic Data Centre contains the crystal structure with the following CCDC number 2262226 (**$K_2(COT^{TMS1})$**), 2262227 (**$K_2(COT^{TMS2})$**), 2262228 (**$K_2(COT^{TMS3})$**), 2262229 (**1**), 2262230 (**2**), and 2262231 (**3**).

Table S4 Crystallographic Data and Structure Refinements for **$K_2(COT^{TMS1})$**, **$K_2(COT^{TMS2})$** and **$K_2(COT^{TMS3})$.**

Complexes	**$K_2(COT^{TMS1})$**	**$K_2(COT^{TMS2})$**	**$K_2(COT^{TMS3})$**
Empirical formula	$C_{19}H_{36}K_2O_4Si$	$C_{22}H_{44}K_2O_4Si_2$	$C_{29}H_{56}K_2O_3Si_3$
Formula weight	434.77	506.95	615.20
Temperature/K	100.00	99.99	100.00
Crystal system	orthorhombic	orthorhombic	orthorhombic
Space group	*P*nma	*P*nma	$P2_12_12_1$
a/Å	16.5310(6)	9.3885(10)	8.6162(3)
b/Å	14.1823(6)	16.5709(9)	20.3535(10)
c/Å	10.1672(4)	18.6126(12)	20.3682(10)
α/°	90	90	90
β/°	90	90	90
γ/°	90	90	90
Volume/Å^3	2383.68(16)	2895.7(4)	3572.0(3)
Z	4	4	4
ρ_{calc}g/cm^3	1.211	1.163	1.144
μ/mm^{-1}	0.467	0.432	0.391
Crystal size/mm^3	0.4 × 0.3 × 0.1	0.4 × 0.4 × 0.1	0.4 × 0.3 × 0.2
Radiation	Mo$K\alpha$ (λ = 0.71073)	Mo$K\alpha$ (λ = 0.71073)	Mo$K\alpha$ (λ = 0.71073)
θ_{min}, θ_{max}, deg	4.928, 55.088	4.916, 54.972	4.474, 55.062
Final *R* indexes [I>=2σ (I)]	R_1 = 0.0334	R_1 = 0.0305	R_1 = 0.0465
Final *R* indexes [all data]	wR_2 = 0.1082	wR_2 = 0.0754	wR_2 = 0.1095

Table S5 Crystallographic Data and Structure Refinements for **1** - **3**

Complexes	**1**	**2**	**3**
Empirical formula	$C_{30}H_{52}ErKO_4Si_2$	$C_{36}H_{67}ErKO_4Si_4$	$C_{60}H_{120}ErKO_{13}Si_6$
Formula weight	739.25	883.62	1424.45
Temperature/K	100.00	100.01	102.99
Crystal system	monoclinic	orthorhombic	monoclinic
Space group	$P2_1/c$	$Fdd2$	$P2_1/n$
a/Å	12.7167(5)	36.8885(14)	9.9662(7)
b/Å	13.3493(5)	38.9549(15)	22.897(3)
c/Å	20.2555(7)	12.4524(5)	33.0980(19)
α/°	90	90	90
β/°	99.8330(10)	90	94.914(4)
γ/°	90	90	90
Volume/Å^3	3388.0(2)	17893.9(12)	7525.0(11)
Z	4	16	4
ρ_{calc}g/cm^3	1.449	1.312	1.257
μ/mm^{-1}	2.701	2.108	1.318
Crystal size/mm^3	0.3 × 0.2 × 0.2	0.6 × 0.2 × 0.2	0.4 × 0.2 × 0.2
Radiation	Mo$K\alpha$ (λ = 0.71073)	Mo$K\alpha$ (λ = 0.71073)	Mo$K\alpha$ (λ = 0.71073)
θ_{min}, θ_{max}, deg	4.666, 55.088	4.772, 61.266	4.544, 55.122
Final R indexes [I>=2σ (I)]	R_1 = 0.0257	R_1 = 0.0211	R_1 = 0.0410
Final R indexes [all data]	wR_2 = 0.0673	wR_2 = 0.0526	wR_2 = 0.1028

Ab Initio Calculations

OpenMolcas [34] was used to perform the CASSCF-SO calculation of the electronic structures of **1-3** with the molecular geometries taken from the crystallographic analyses; no optimization was made except for taking the largest disorder component. Relativistic effects have been accounted for by using the 2nd order Douglas-Kroll Hess Hamiltonian, and the basis sets from ANO-RCC library [35-36] were accordingly employed, with VTZP quality for Er atoms, VDZP quality for the coordinating C atoms, and VDZ quality for any remaining atoms. Cholesky decomposition of the two-electron integrals with a threshold of 10^{-8} was performed to save disk space and to reduce computational demand. The molecular orbitals were optimized in state-averaged CASSCF calculations within each spin manifold, with a minimal active space of 11 electrons in 7 orbitals and considering 35 and 112 roots for spin quartet and doublet, respectively. For each spin multiplicity, the number of states mixed by spin orbit coupling are also 35 and 112, respectively. The resulting spin-orbit wavefunctions were decomposed into their CF wavefunctions, and the magnetic susceptibility was calculated using SINGLE_ANISO [37].

Table S6. Electronic structure of **1** calculated with the crystal field parameters obtained from CASSCF-SO at the crystal structure. Each row corresponds to a Kramers doublet. Last column reports the original CASSCF-SO energies.

Energy (cm^{-1})	**Energy (K)**	g_x	g_y	g_z	**Wavefunction**
0.00	0.00	1.14×10^{-5}	1.60×10^{-5}	17.94	$99.9\%\|\pm 15/2\rangle$
126.09	181.32	10.07	9.05	1.22	$99.5\%\|\pm 1/2\rangle$
197.22	283.60	0.17	0.26	11.00	$61.6\%\|\pm 13/2\rangle + 37.3\%\|\pm 3/2\rangle$
208.05	299.18	0.22	0.40	8.20	$61.3\%\|\pm 3/2\rangle + 38.0\%\|\pm 13/2\rangle$
327.74	471.29	0.06	0.19	6.11	$97.5\%\|\pm 5/2\rangle$
393.11	565.29	0.005	0.008	12.85	$94.1\%\|\pm 11/2\rangle + 5.3\ \%\|\pm 7/2\rangle$
445.82	641.09	0.03	0.12	8.77	$92.4\%\|\pm 7/2\rangle + 5.6\%\|\pm 11/2\rangle$
480.92	691.56	0.04	0.10	10.82	$97.5\%\|\pm 9/2\rangle$

Table S7. Electronic structure of **2** calculated with the crystal field parameters obtained from CASSCF-SO at the crystal structure. Each row corresponds to a Kramers doublet. Last column reports the original CASSCF-SO energies.

Energy (cm^{-1})	Energy (K)	g_x	g_y	g_z	Wavefunction
0.00	0.00	1.30×10^{-4}	1.44×10^{-4}	17.94	99.8%| ± 15/2⟩
150.69	216.69	10.34	8.76	1.22	99.0%| ± 1/2⟩
180.80	259.99	0.07	0.08	15.20	97.0%| ± 13/2⟩ + 2.5%| ± 3/2⟩
227.75	327.50	0.49	0.95	3.97	96.2%| ± 3/2⟩ +2.6%| ± 13/2⟩
344.91	495.98	0.02	0.46	6.10	97.9%| ± 5/2⟩
378.76	544.66	0.04	0.04	12.99	97.2%| ± 11/2⟩ + 1.7 %| ± 7/2⟩
451.93	649.88	0.11	0.44	8.51	95.5%| ± 7/2⟩ + 1.8%| ± 11/2⟩
476.14	684.69	0.20	0.35	10.74	98.7%| ± 9/2⟩

Table S8. Electronic structure of **3** calculated with the crystal field parameters obtained from CASSCF-SO at the crystal structure. Each row corresponds to a Kramers doublet. Last column reports the original CASSCF-SO energies.

Energy (cm^{-1})	Energy (K)	g_x	g_y	g_z	Wavefunction
0.00	0.00	4.75×10^{-4}	1.38×10^{-3}	17.90	99.3%| ± 15/2⟩
126.59	181.32	9.99	9.02	1.30	97%| ± 1/2⟩ + 1.1%| ± 3/2⟩
165.94	283.60	0.23	0.27	13.13	79.1%| ± 13/2⟩ + 18.6%| ± 3/2⟩
205.46	299.18	0.11	0.40	6.00	78.5%| ± 3/2⟩ + 29.3%| ± 13/2⟩
306.33	471.29	0.24	0.62	6.31	92.4%| ± 5/2⟩ + 2.7%| ± 7/2⟩
352.92	565.29	0.14	0.21	12.78	94.3%| ± 11/2⟩ + 2.9 %| ± 7/2⟩
403.93	641.09	0.08	0.51	10.75	75%| ± 7/2⟩ + 22.2%| ± 9/2⟩
448.05	691.56	0.16	0.27	13.94	75.3%| ± 9/2⟩ + 19.7%| ± 7/2⟩

Magnetic Studies

Magnetic susceptibility measurements were carried out with a Quantum Design MPMS-3 SQUID magnetometer in a field of 0.1 T and at between 2 and 300 K. In a typical measurement, a polycrystalline sample was sealed with melted eicosane in an NMR tube under vacuum. The standard AC magnetic susceptibility data collected with a 3.5-Oe oscillating AC field.

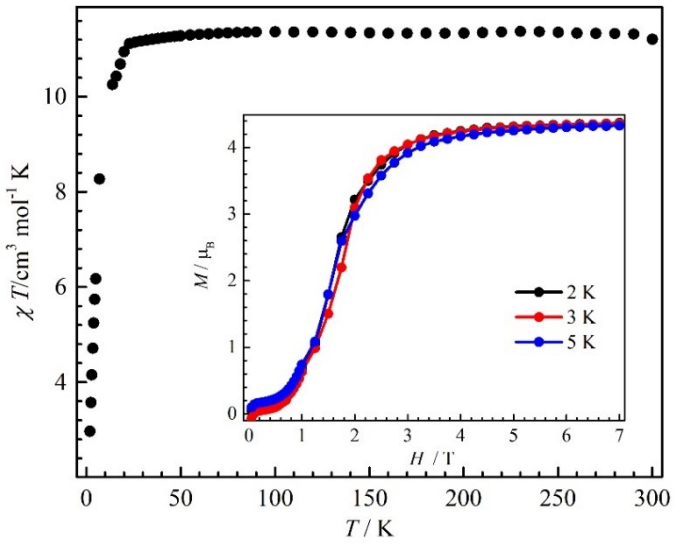

Figure S2 The χT versus T plot of **1** under 1000 Oe dc field. Inset: The field-dependent magnetization plots at indicated temperatures.

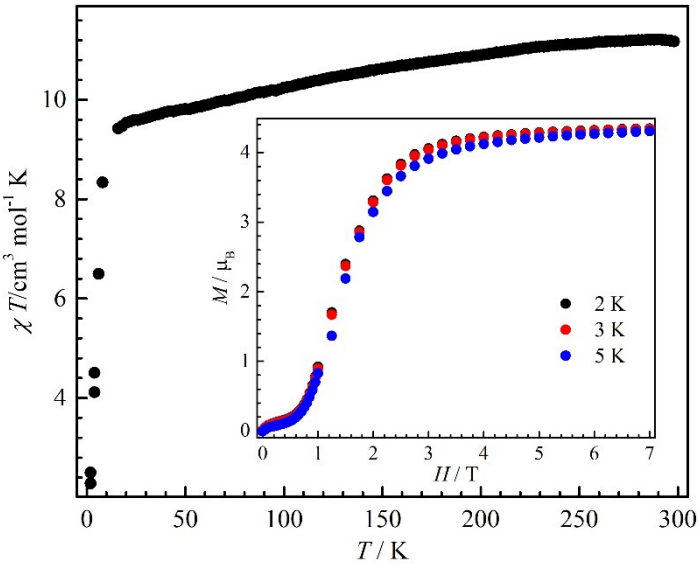

Figure S3 The χT versus T plot of **2** under 1000 Oe dc field. Inset: The field-dependent magnetization plots at indicated temperatures.

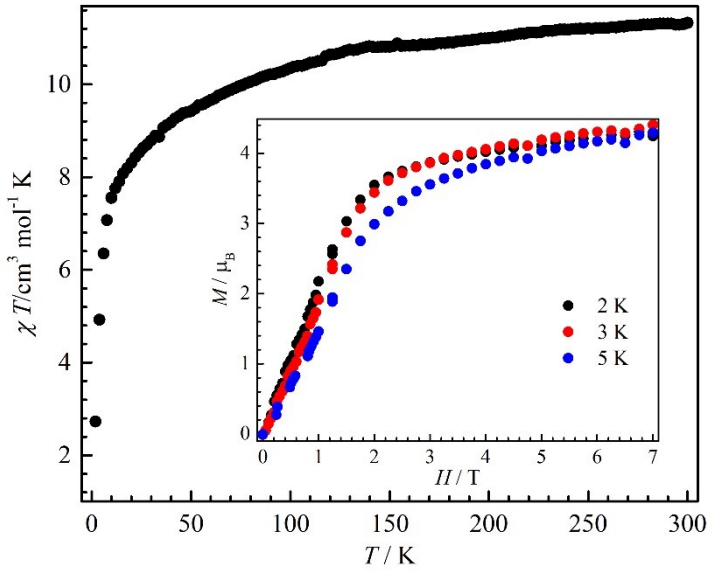

Figure S4 The χT versus T plot of **3** under 1000 Oe dc field. Inset: The field-dependent magnetization plots at indicated temperatures.

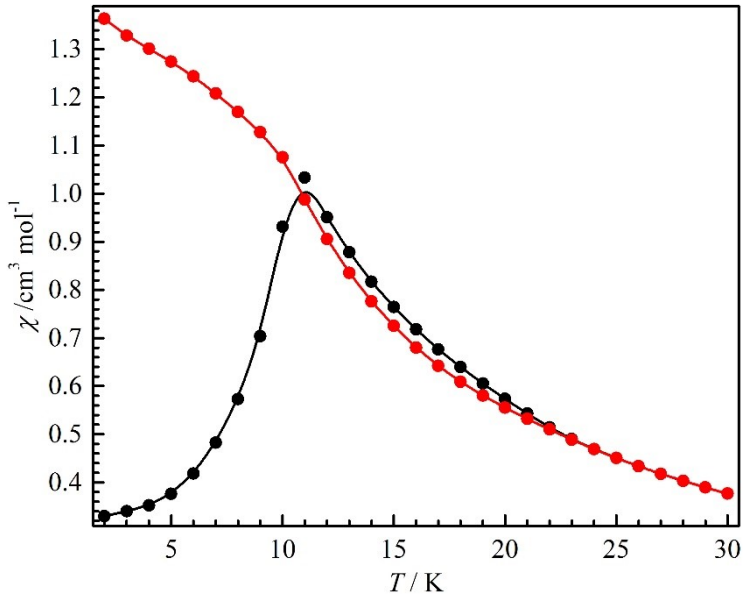

Figure S5 Field-cooled (FC) and zero-field-cooled (ZFC) magnetization data for **1**. Solid lines are guides for vision.

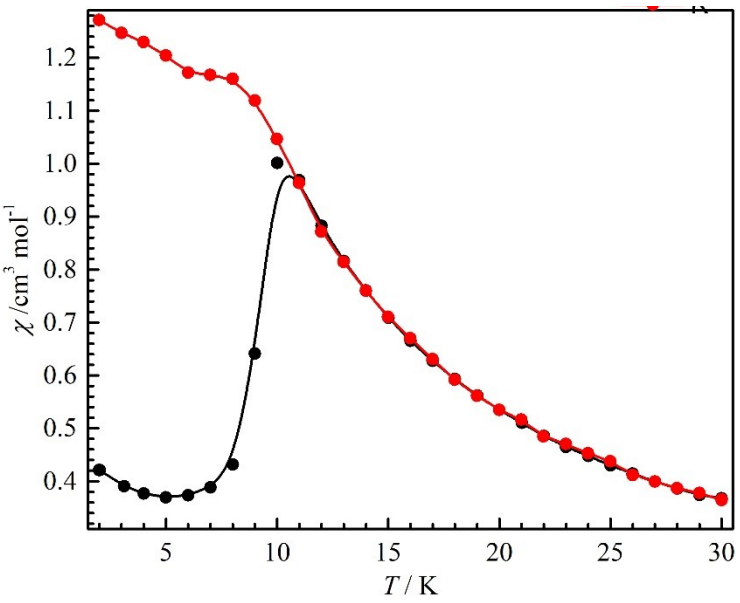

Figure S6 Field-cooled (FC) and zero-field-cooled (ZFC) magnetization data for **2**. Solid lines are guides for vision.

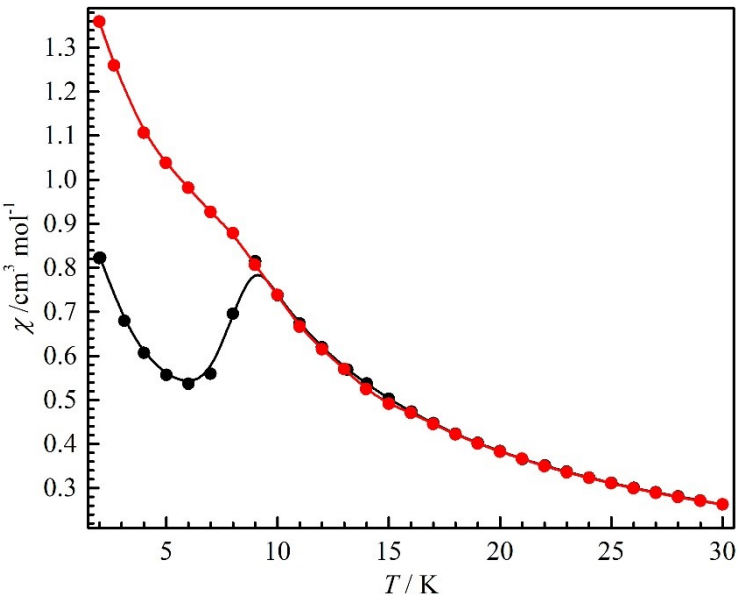

Figure S7 Field-cooled (FC) and zero-field-cooled (ZFC) magnetization data for **3**. Solid lines are guides for vision.

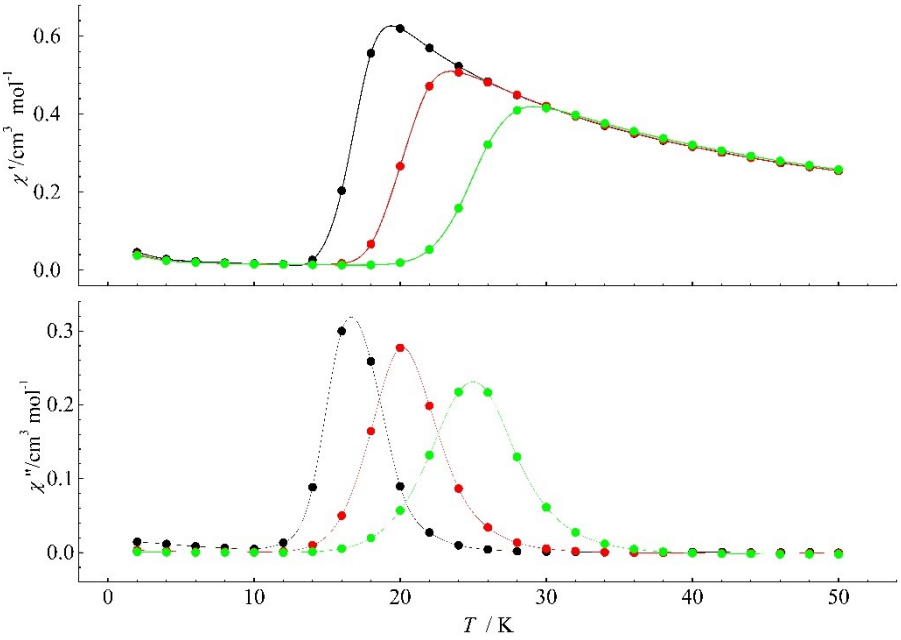

Figure S8 Temperature-dependence of the in-phase (χ', top) and out-of-phase (χ'', bottom) AC susceptibility signals under zero DC field by standard AC susceptibility measurements for **1** at frequencies of 7 Hz (black), 77 Hz (red) and 777 Hz (green). Solid lines are guide for vision.

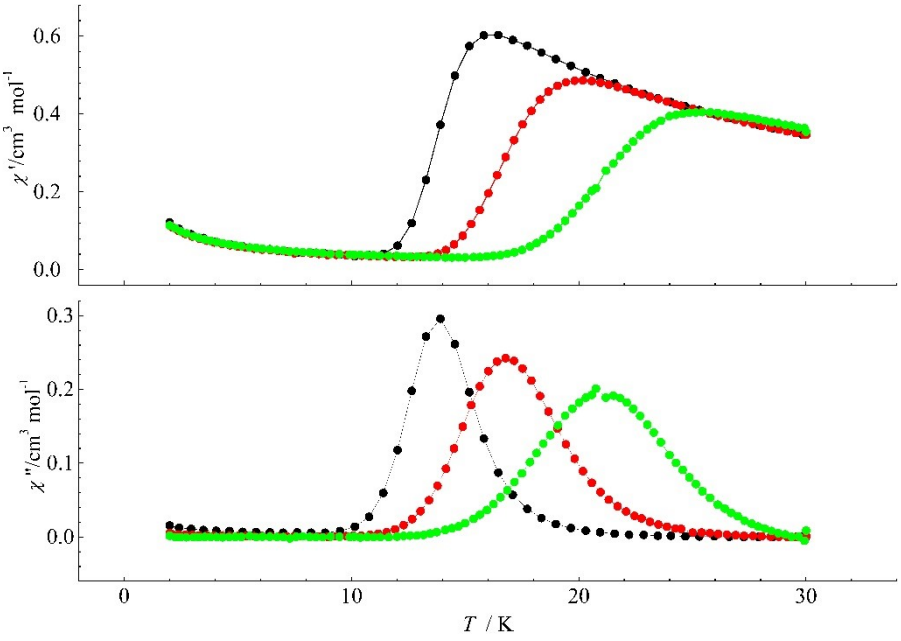

Figure S9 Temperature-dependence of the in-phase (χ', top) and out-of-phase (χ'', bottom) AC susceptibility signals under zero DC field by standard AC susceptibility measurements for **2** at frequencies of 7 Hz (black), 77 Hz (red) and 777 Hz (green). Solid lines are guide for vision.

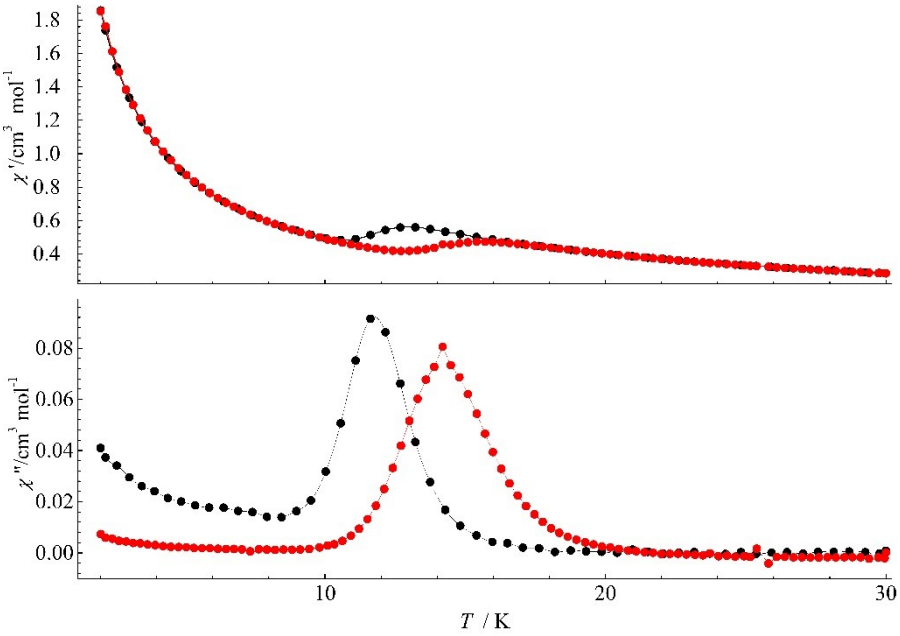

Figure S10 Temperature-dependence of the in-phase (χ', top) and out-of-phase (χ'', bottom) AC susceptibility signals under zero DC field by standard AC susceptibility measurements for **3** at frequencies of 7 Hz (black) and 77 Hz (red). Solid lines are guide for vision.

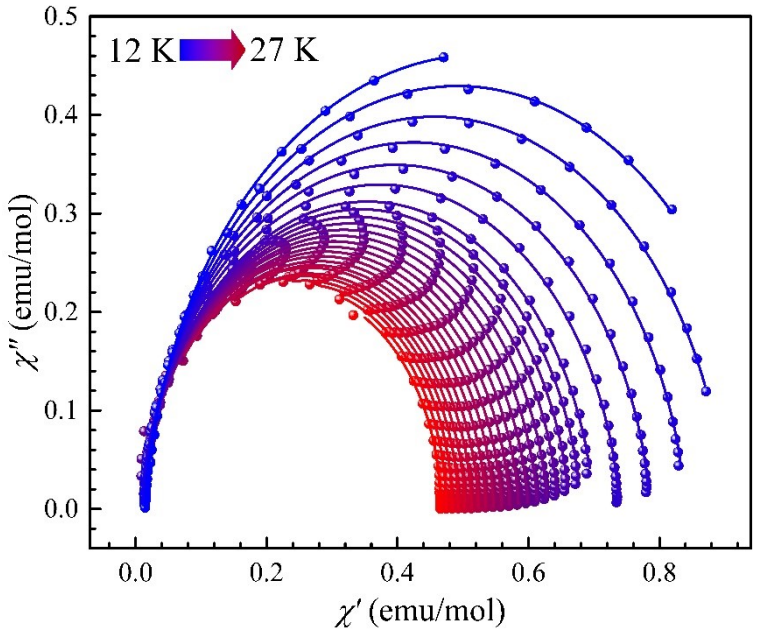

Figure S11 Cole–Cole plots using the frequency-dependence ac susceptibility data under the zero dc field for **1** from 12 K (blue) to 27 K (red). The solid lines are the best fits.

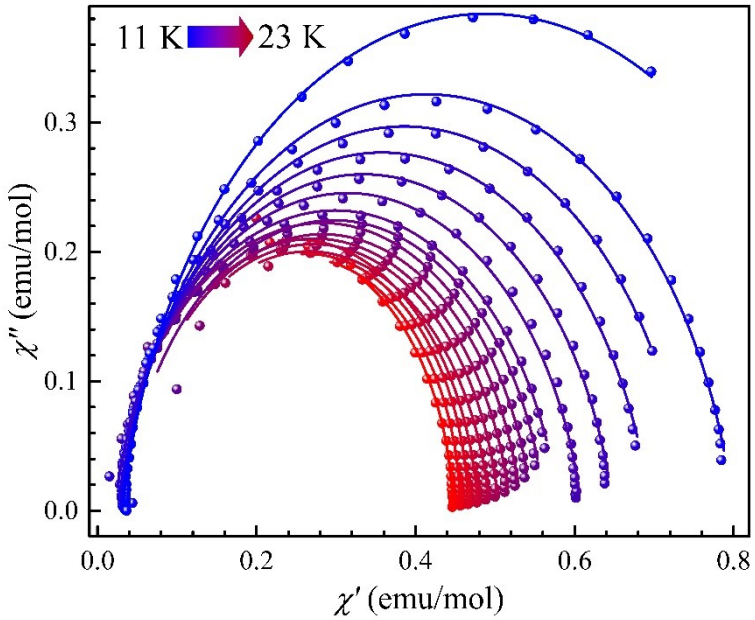

Figure S12 Cole–Cole plots using the frequency-dependence ac susceptibility data under the zero dc field for **2** from 11 K (blue) to 23 K (red). The solid lines are the best fits.

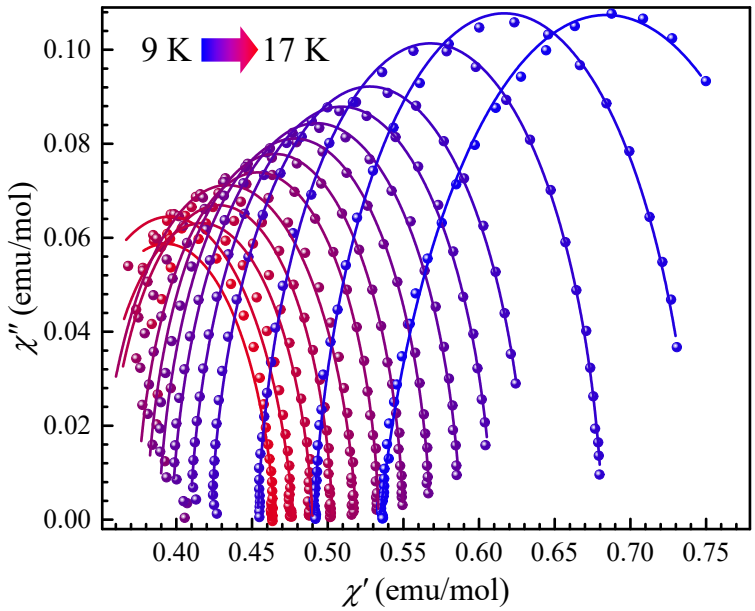

Figure S13 Cole–Cole plots using the frequency-dependence ac susceptibility data under the zero dc field for **3** from 9 K (blue) to 17 K (red). The solid lines are the best fits.

Table S9 Relaxation fitting parameters obtained using a generalized Debye model for **1** from 27 K to 12 K under zero dc field, fitted with the waveform module as implemented in CCFIT2.

T / K	τ / s	τ_err	α
27	1.06646E-4	5.41243E-6	0
26.5	1.28812E-4	2.95016E-6	7.35444E-4
26	1.59788E-4	3.40453E-6	1.64573E-4
25.5	1.94012E-4	2.95885E-6	0.00734
25	2.33317E-4	2.08517E-6	0.0183
24.5	2.8995E-4	2.01837E-6	0.02184
24	3.52685E-4	2.69955E-6	0.03131
23.5	4.42302E-4	1.91214E-6	0.03499
23	5.55059E-4	2.26681E-6	0.0387
22.5	6.93842E-4	2.83885E-6	0.04573
22	8.82589E-4	3.08535E-6	0.04791
21.5	0.00113	3.5054E-6	0.05073
21	0.00144	5.88952E-6	0.05687
20.5	0.00188	6.48972E-6	0.05613
20	0.00246	8.82654E-6	0.06009
19.5	0.00326	1.05618E-5	0.06071
19	0.00435	1.44209E-5	0.06357
18.5	0.00589	2.02534E-5	0.06352
18	0.00809	2.76747E-5	0.06536
17	0.01585	6.21672E-5	0.0672
16	0.03377	1.22191E-4	0.06913
15	0.07891	2.75726E-4	0.07105
14	0.20421	6.96632E-4	0.07295
13	0.5842	0.00211	0.07083
12	1.7909	0.06509	0.00997

Table S10 Relaxation fitting parameters obtained using a generalized Debye model for **2** from 24 K to 11 K under zero dc field, fitted with the waveform module as implemented in CCFIT2.

T / K	τ / s	τ_err	α
23	1.07842E-4	6.78278E-6	0.02425
22.5	1.49595E-4	1.02803E-5	0.00821
22	1.86232E-4	1.17676E-5	0.05809
21.5	1.98836E-4	1.00544E-5	0.05809
21	2.52186E-4	2.95885E-6	0.00734
20.5	3.251E-4	4.52482E-6	0.07943
20	3.98529E-4	5.6993E-6	0.10194
19.5	5.2858E-4	7.34195E-6	0.09977
19	6.71548E-4	9.21223E-6	0.1097
18.5	9.1751E-4	1.38009E-5	0.10678
18	0.00119	8.92652E-6	0.12365
17	0.00223	1.45231E-5	0.11589
16	0.00456	2.35033E-5	0.11904
15	0.01018	5.91089E-5	0.12505
14	0.02544	1.82772E-4	0.12247
13	0.07019	3.79463E-4	0.11439
11	0.83004	0.01332	0.11166

Table S11 Relaxation fitting parameters obtained using a generalized Debye model for **3** from 18 K to 8 K under zero dc field, fitted with the waveform module as implemented in CCFIT2.

T / K	τ / s	τ_err	α
17	2.38299E-4	2.18928E-5	0.13101
16.5	3.04248E-4	2.6967E-5	0.15307
16	5.45331E-4	2.58798E-5	0.09739
15.5	8.20836E-4	2.92002E-5	0.07386
15	0.00109	6.08788E-5	0.11492
14.5	0.00187	4.84428E-5	0.05054
14	0.00283	6.50209E-5	0.05494
13.5	0.00439	7.0078E-5	0.06465
13	0.00705	5.72535E-5	0.07928
12.5	0.01172	6.75337E-5	0.08227
12	0.02053	1.33141E-4	0.08212
11	0.06574	2.85588E-4	0.07485
10	0.2222	0.00111	0.09915
9	0.75414	0.01016	0.20747

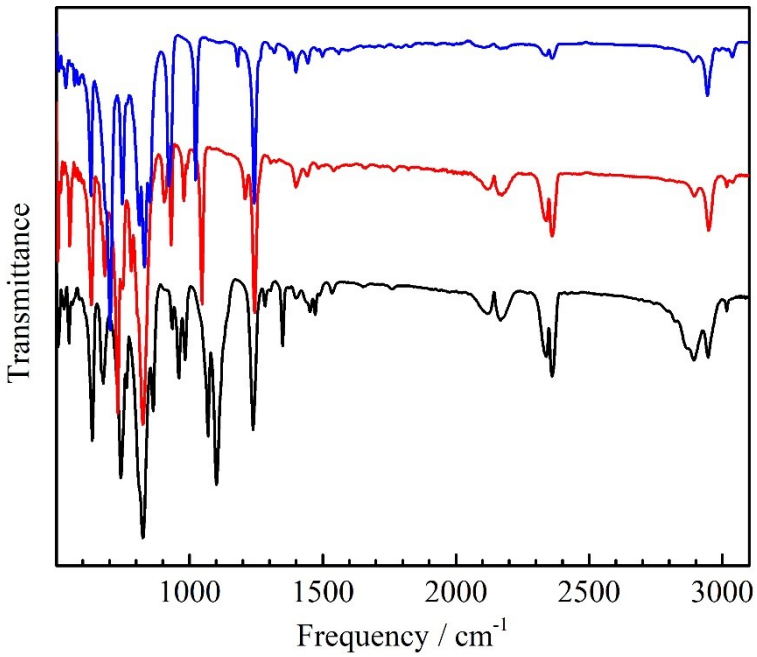

Figure S14 Comparison of IR spectra for **1** (blue), **2** (red) and **3** (black).

Table S12 Experimental IR Absorption Frequencies (cm^{-1}) and Vibrational Assignments for **1**-**3**.

Absorption Frequencies / cm^{-1}			Vibrational assignment
1	**2**	**3**	
630	631 682	634 677	TMS Si–C stretch [39]
702 748	731	744	out-of-plane C–H bend + C–H bend (TMS) [39]
811 831	825	825 863	C–H bend (TMS) [39]
925	931	935	CCH bend (COT) [39]
	979	960 983	sym Si–C stretch [39]
1023	1047	1069	asym Si–C stretch [39]
-	-	1102	C–O stretch (18-C-6) [40]
1181	1210	-	C–C stretch (COT) [39]
-	-	1350 1402 1452	C–H bend (18-C-6) [40]
1243	1244	1239	CH_3 umbrella [39]
2362 2335	2362 2337	2362 2336	CO_2 contaminant
2892 2944	2895 2949	2892 2946	C–H stretch (alkane) [39]
3037	3038	3016	C–H stretch (COT) [39]

REFERENCES

[1] K. R. Meihaus and J. R. Long, *J. Am. Chem. Soc.*, 2013, **135**, 17952-17957.

[2] T.-J. Xue, Y.-S. Ding, D. Reta, Q.-W. Chen, X. Zhu and Z. Zheng, *Cryst. Growth Des.*, 2023, **23**, 565-573.

[3] (a) S. D. Jiang, B. W. Wang, H. L. Sun, Z. M. Wang and S. Gao, *J. Am. Chem. Soc.*, 2011, **133**, 4730-4733. (b) S.-D. Jiang, S.-S. Liu, L.-N. Zhou, B.-W. Wang, Z.-M. Wang and S. Gao, *Inorg. Chem.*, 2012, **51**, 3079-3087.

[4] L. Ungur, J. J. Le Roy, I. Korobkov, M. Murugesu and L. F. Chibotaru, *Angew. Chem. Int. Ed.*, 2014, **53**, 4413-4417.

[5] J. J. Le Roy, L. Ungur, I. Korobkov, L. F. Chibotaru and M. Murugesu, *J. Am. Chem. Soc.*, 2014, **136**, 8003-8010.

[6] Y. S. Meng, C. H. Wang, Y. Q. Zhang, X. B. Leng, B. W. Wang, Y. F. Chen and S. Gao, *Inorg. Chem. Front.*, 2016, **3**, 828-835.

[7] J. D. Hilgar, B. S. Flores and J. D. Rinehart, *Chem. Commun.*, 2017, **53**, 7322-7324.

[8] M. He, X. Chen, T. Bodenstein, A. Nyvang, S. F. M. Schmidt, Y. Peng, E. Moreno-Pineda, M. Ruben, K. Fink, M. T. Gamer, A. K. Powell and P. W. Roesky, *Organometallics*, 2018, **37**, 3708-3717.

[9] S. M. Chen, J. Xiong, Y. Q. Zhang, Q. Yuan, B. W. Wang and S. Gao, *Chem. Sci.*, 2018, **9**, 7540-7545.

[10] J. D. Hilgar, M. G. Bernbeck, B. S. Flores and J. D. Rinehart, *Chem. Sci.*, 2018, **9**, 7204-7209.

[11] J. D. Hilgar, M. G. Bernbeck and J. D. Rinehart, *J. Am. Chem. Soc.*, 2019, **141**, 1913-1917.

[12] Y.-S. Meng, M.-W. Yang, L. Xu, J. Xiong, J.-Y. Hu, T. Liu, B.-W. Wang and S. Gao, *Dalton Trans.,* 2019, **48**, 10407-10411.

[13] L. Munzfeld, C. Schoo, S. Bestgen, E. Moreno-Pineda, R. Koppe, M. Ruben and P. W. Roesky, *Nat. Commun.*, 2019, **10**. 3135.

[14] M. G. Bernbeck, J. D. Hilgar and J. D. Rinehart, *Polyhedron*, 2020, **175**. 114206.

[15] D. Z. Zhu, M. M. Wang, L. L. Guo, W. Shi, J. F. Li and C. M. Cui, *Organometallics*, 2021, **40**, 2394-2399.

[16] Z. Zhou, J. McNeely, J. Greenough, Z. Wei, H. Han, M. Rouzières, A. Y. Rogachev, R. Clérac and M. A. Petrukhina, *Chem. Sci.*, 2022, **13**, 3864-3874.

[17] M. D. Korzyński, M. Bernhardt, V. Romankov, J. Dreiser, G. Matmon, F. Pointillart, B. Le Guennic, O. Cador and C. Copéret, *Chem. Sci*, 2022., **13**, 10574-10580.

[18] L. Münzfeld, M. Dahlen, A. Hauser, N. Mahieu, S. K. Kuppusamy, J. Moutet, M. Tricoire, R. Köppe, L. La Droitte, O. Cador, B. Le Guennic, G. Nocton, E. Moreno-Pineda, M. Ruben and P. W. Roesky, *Angew. Chem. Int. Ed.*, 2023, e202218107.

[19] J. J. Le Roy, I. Korobkov and M. Murugesu, *Chem. Commun.*, 2014, **50**, 1602-1604.

[20] L. Münzfeld, X. Sun, S. Schlittenhardt, C. Schoo, A. Hauser, S. Gillhuber, F. Weigend, M. Ruben and P. W. Roesky, *Chem. Sci.*, 2022, **13**, 945-954.

[21] A. P. Orlova, J. D. Hilgar, M. G. Bernbeck, M. Gembicky and J. D. Rinehart, *J. Am. Chem. Soc.*, 2022, **144**, 11316-11325.

[22] J. D. Hilgar, A. K. Butts and J. D. Rinehart, *Phys. Chem. Chem. Phys.*, 2019, **21**, 22302-22307.

[23] W. Huang, B. M. Upton, S. I. Khan and P. L. Diaconescu, *Organometallics*, 2013, **32**, 1379-1386.

[24] S. Majumder and A. L. Odom, *Tetrahedron Lett.*, 2008, **49**, 1771-1772.

[25] J. Gasteiger, G. E. Gream, R. Huisgen, W. E. Konz and U. Schnegg, *Chem. Ber.*, 1971, **104**, 2412-2419.

[26] A. de Meijere, C.-H. Lee, B. Bengtson, E. Pohl, S. I. Kozhushkov, P. R. Schreiner, R. Boese and T. Haumann, *Chem-Eur. J.*, 2003, **9**, 5481-5488.

[27] N. C. Burton, F. G. N. Cloke, S. C. P. Joseph, H. Karamallakis and A. A. Sameh, *J. Organomet. Chem.*, 1993, **462**, 39-43.

[28] T. J. Katz, *J. Am. Chem. Soc.*, 1960, **82**, 3784-3785.

[29] V. Lorenz, P. Liebing, J. Rausch, S. Blaurock, C. G. Hrib, L. Hilfert and F. T. Edelmann, *J. Organomet. Chem.*, 2018, **857**, 38-44.

[30] V. Lorenz, P. Liebing, A. Bathelier, F. Engelhardt, L. Maron, L. Hilfert, S. Busse and F. T. Edelmann, *Chem Commun*, 2018, **54**, 10280-10283.

[31] O. V. Dolomanov, L. J. Bourhis, R. J. Gildea, J. A. K. Howard and H. Puschmann, *J. Appl. Cryst.,* 2009, **42**, 339-341.

[32] G. Sheldrick, *Acta. Cryst. A.,* **2015**, *71*, 3-8.

[33] G. Sheldrick, *Acta. Cryst. C*, 2015, **71**, 3-8.

[34] G. Li Manni, I. Fdez. Galván, A. Alavi, F. Aleotti, F. Aquilante, J. Autschbach, D. Avagliano, A. Baiardi, J. J. Bao, S. Battaglia, L. Birnoschi, A. Blanco-González, S. I. Bokarev, R. Broer, R. Cacciari, P. B. Calio, R. K. Carlson, R. Carvalho Couto, L. Cerdán, L. F. Chibotaru, N. F. Chilton, J. R. Church, I. Conti, S. Coriani, J. Cuéllar-Zuquin, R. E. Daoud, N. Dattani, P. Decleva, C. de Graaf, M. G. Delcey, L. De Vico, W. Dobrautz, S. S. Dong, R. Feng, N. Ferré, M. Filatov, L. Gagliardi, M. Garavelli, L. González, Y. Guan, M. Guo, M. R. Hennefarth, M. R. Hermes, C. E. Hoyer, M. Huix-Rotllant, V. K. Jaiswal, A. Kaiser, D. S. Kaliakin, M. Khamesian, D. S. King, V. Kochetov, M. Krośnicki, A. A. Kumaar, E. D. Larsson, S. Lehtola, M.-B. Lepetit, H. Lischka, P. López Ríos, M. Lundberg, D. Ma, S. Mai, P. Marquetand, I. C. D. Merritt, F. Montorsi, M. Mörchen, A. Nenov, V. H. A. Nguyen, Y. Nishimoto, M. S. Oakley, M. Olivucci, M. Oppel, D. Padula, R. Pandharkar, Q. M. Phung, F. Plasser, G. Raggi, E. Rebolini, M. Reiher, I. Rivalta, D. Roca-Sanjuán, T. Romig, A. A. Safari, A. Sánchez-Mansilla, A. M. Sand, I. Schapiro, T. R. Scott, J. Segarra-Martí, F. Segatta, D.-C. Sergentu, P. Sharma, R. Shepard, Y. Shu, J. K. Staab, T. P. Straatsma, L. K. Sørensen, B. N. C. Tenorio, D. G. Truhlar, L. Ungur, M. Vacher, V. Veryazov, T. A. Voß, O. Weser, D. Wu, X. Yang, D. Yarkony, C. Zhou, J. P. Zobel and R. Lindh, *J. Chem. Theory. Comput.*, 2023, DOI: 10.1021/acs.jctc.3c00182.

[35] B. O. Roos, R. Lindh, P. A. Malmqvist, V. Veryazov and P. O. Widmark, *J Phys Chem A*, 2004, **108**, 2851-2858.

[36] B. O. Roos, R. Lindh, P. A. Malmqvist, V. Veryazov and P. O. Widmark, *J Phys Chem A*, 2005, **109**, 6575-6579.

[37] L. Ungur and L. F. Chibotaru, *Chem-Eur J*, 2017, **23**, 3708-3718.

[38] D. Reta and N. F. Chilton, *Phys Chem Chem Phys*, 2019, **21**, 23567-23575.

[39] T. Tsuji, N. Hosoya, S. Fukazawa, R. Sugiyama, T. Iwasa, H. Tsunoyama, H. Hamaki, N. Tokitoh and A. Nakajima, *J. Phys. Chem. C*, 2014, **118**, 5896-5907.

[40] G. W. Gokel, D. J. Cram, C. L. Liotta, H. P. Harris and F. L. Cook, *J. Org. Chem.*, 1974, **39**, 2445-2446.